

Hydrothermal Flow Variability: Two New Potential Measurement Techniques

Timothy J. Crone, William S. D. Wilcock, and Russ E. McDuff
School of Oceanography, University of Washington
Box 357940, Seattle, WA, USA



Introduction

Mid-Ocean ridge hydrothermal systems support rich communities of chemosynthetic organisms and are conduits for large heat and chemical exchanges between young oceanic lithosphere and the ocean. On a global scale, the time-averaged hydrothermal heat flux and many chemical fluxes are well constrained [Elderfield & Schultz, 1996]. On local scales however, these fluxes are clearly temporally and spatially variable [Baker, 1994], but are poorly quantified in large part because there are few time-series measurements of fluid flow with which to integrate temperature and chemical observations.

While time-series measurements of flow have been obtained in low-temperature vents [Pruis & Johnson, 2004; Schultz, et. al., 1996], and point measurements have been obtained in black smokers [Converse, et. al., 1984; Bemis, et. al., 1993], no time-series measurements of black smoker flow exist. High temperatures, low pH, and mineral precipitation limit the long-term effectiveness of invasive flow measurement techniques commonly employed in these environments.

To help fill this data gap, we are working to develop two non-invasive black smoker flow measurement techniques. The first technique capitalizes on the potential for fluid flow to produce sound. Passive acoustic measurements near black smokers could provide flow rate information if such sounds can be detected, and if a relationship between flow rate and acoustic output can be established. Our initial work on this technique shows that black smokers generate considerable acoustic energy and have complex acoustic signatures containing a broadband signal and narrowband tones. The broadband signal power is tidally modulated which likely reflects flow rate variations induced by tidal pumping.

The second technique uses video image analysis to track the motions of plume billows across video image frames. The cross-correlation of video subimages between successive frames yields a two-dimensional representation of the velocity field in the imaged flow. We are working to determine if a transformation can be applied to convert these image-velocity fields into true velocities and discharge rates. Our initial work on this technique shows that plausible image-velocity distributions can be obtained through image correlation velocimetry.

Black Smoker Acoustics

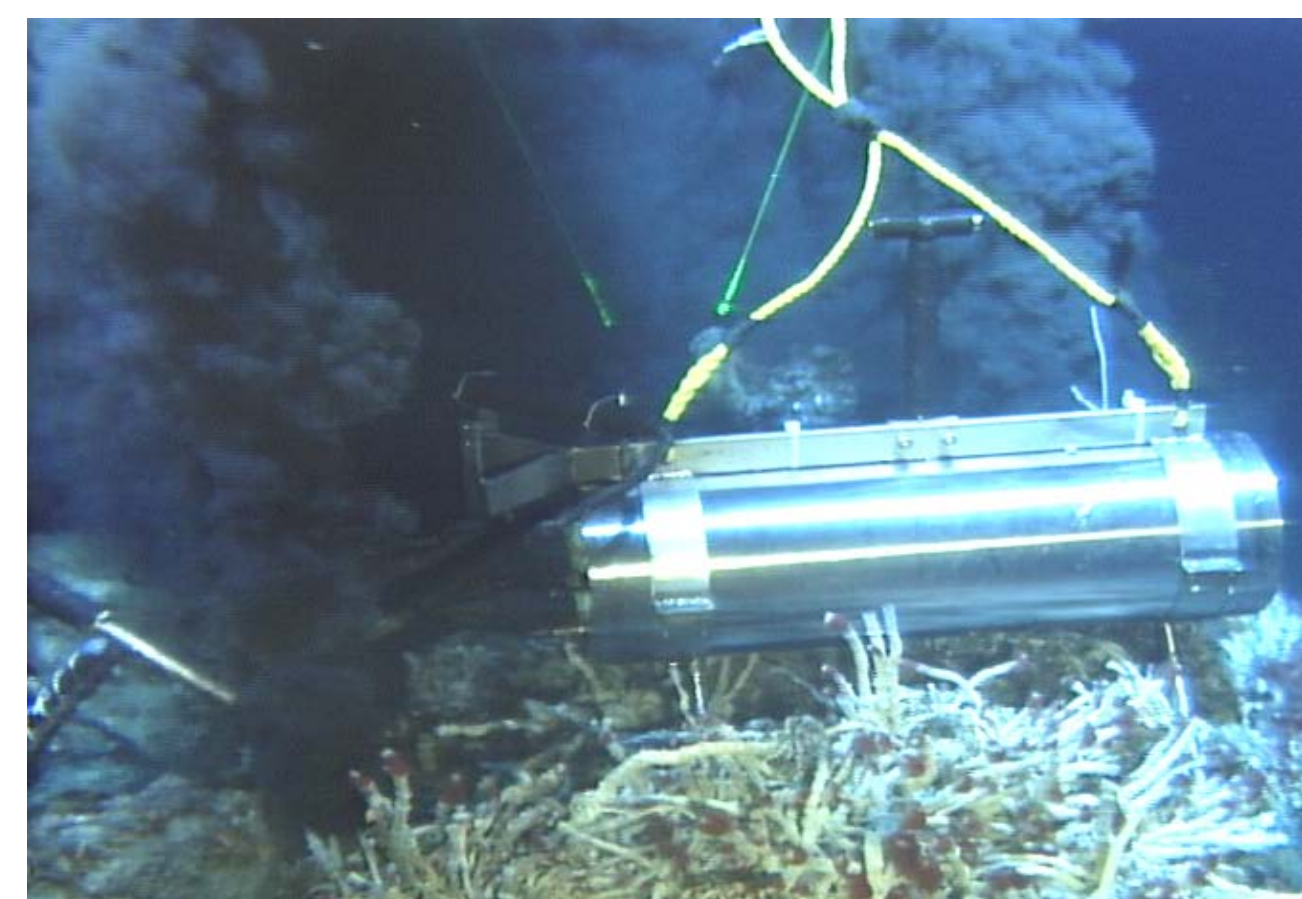


Figure 1. Photograph of the digital acoustic recording system deployed at the Sully vent in September of 2004. We collected ~48 h of sound data from this vent in 2004 and ~136 h of data from the Puffer vent in 2005. Each year we deployed the system several tens of meters away from the vents to record the ambient noise levels.

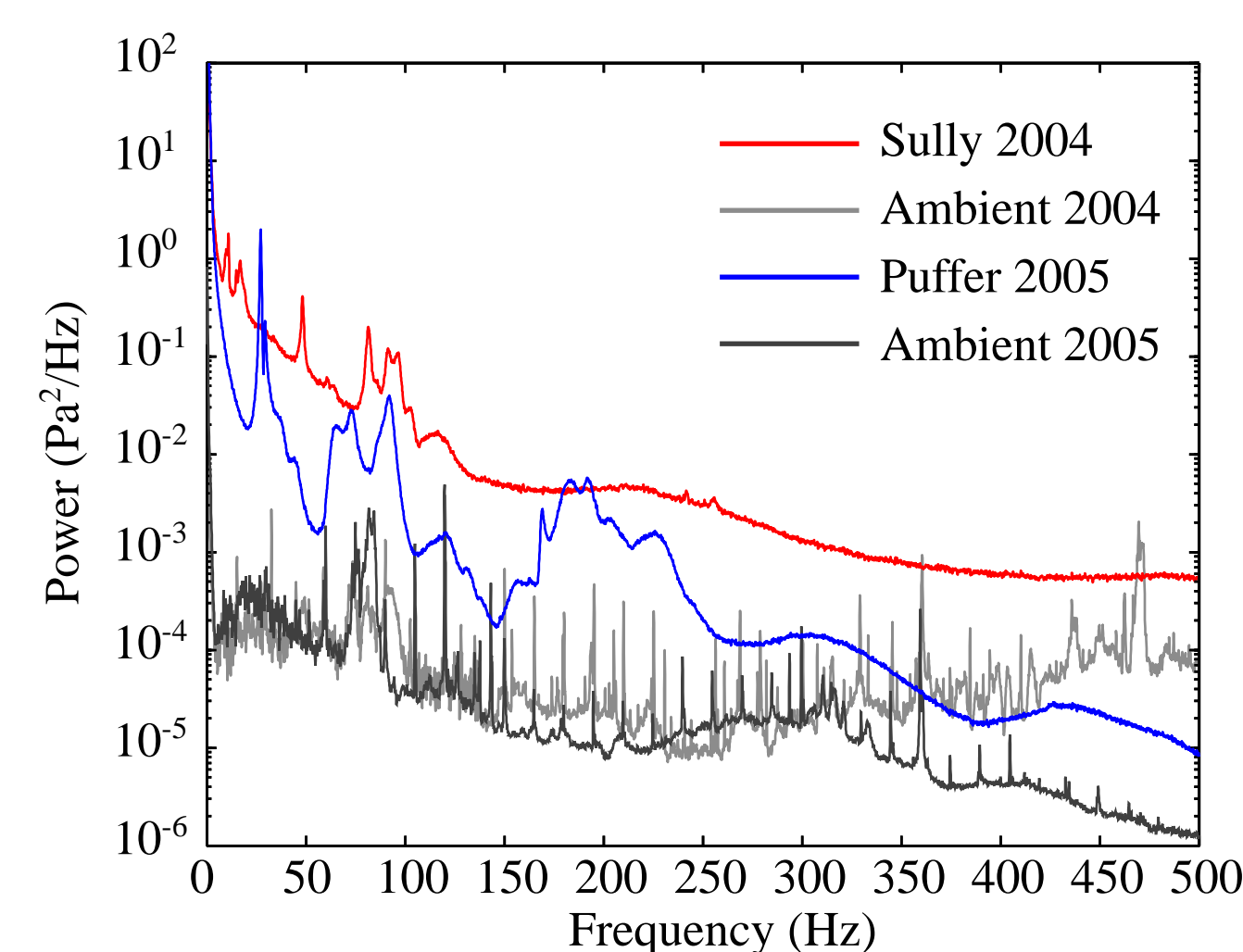


Figure 2. Typical hour-average power spectra for the Sully vent in 2004 and the Puffer vent in 2005. Also shown are the spectra of the ambient noise recordings. Sharp peaks on the ambient curves are associated with ship noise. Both Sully and Puffer radiate broadband acoustic energy at levels significantly higher than background at all measured frequencies. Their spectra also contain sharp peaks at distinct frequencies. Different source mechanisms are likely responsible for the broadband and the narrowband signals. In some frequency bands, acoustic power levels are 30 dB higher than background. Depending on the sound source mechanism vent sounds may be detectable ~5-15 m from the vent orifice.

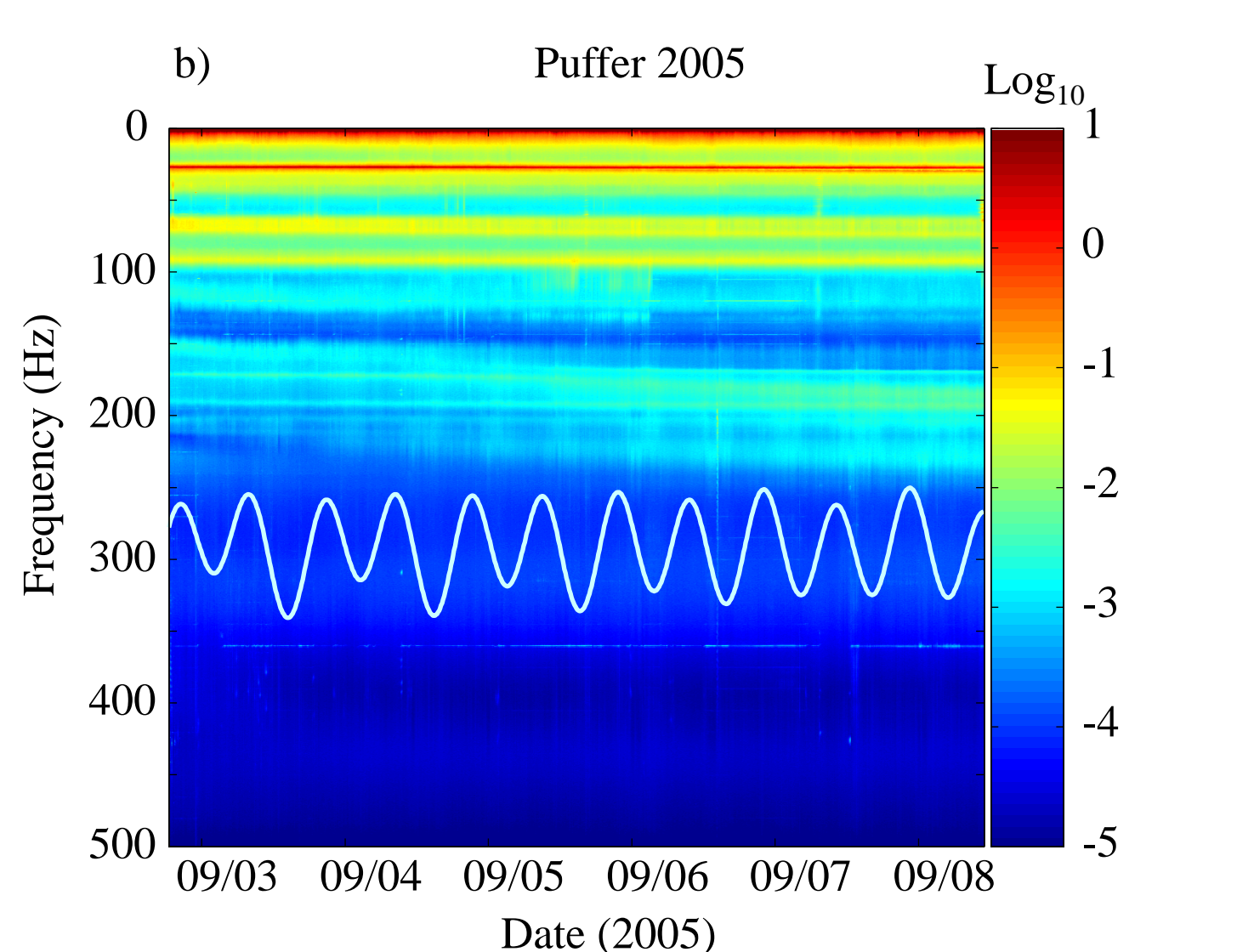


Figure 3. Spectrogram showing the temporal evolution of Puffer's acoustic spectrum. The light blue trace depicts the predicted tidal heights (~1 m amplitude) plotted on an arbitrary scale [Mofjeld, et. al., 1995]. The broad-band signal and the narrow-band peaks vary in time. Peaks are observed to wander, consolidate, and split in two. The broadband signal in certain frequency bands displays tidal modulation. Maximal sound intensity lags high tide by ~125°. Numerical models predict a similar lag for flow rate [Crone & Wilcock, 2005; Jupp & Schultz, 2004].

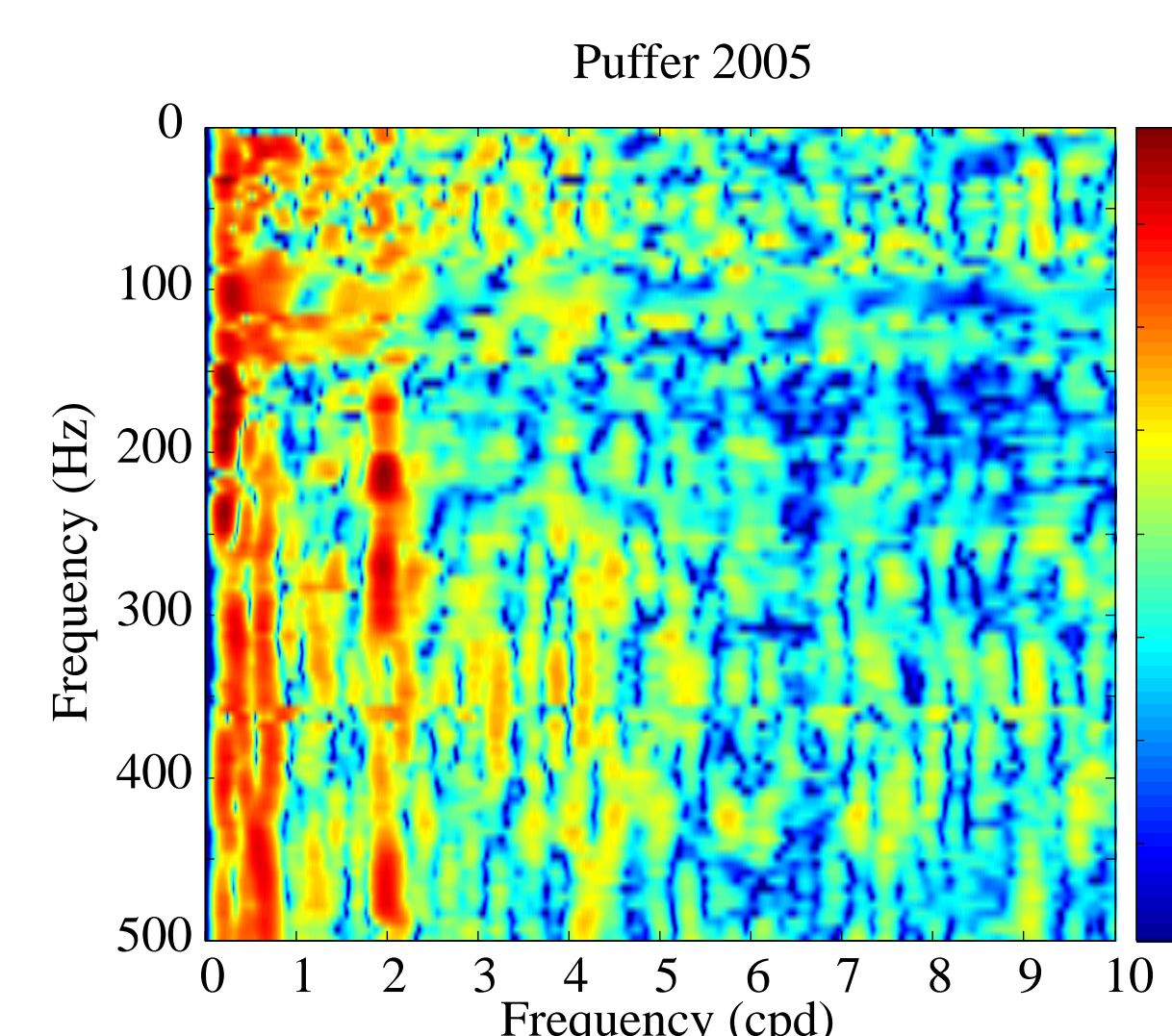


Figure 4. Shaded contours of the normalized power spectral density computed from the time-series of acoustic intensity in different frequency bands from the Puffer 2005 data. Within certain frequency bands, Puffer's acoustic intensity is periodic at semi-diurnal frequencies, which is likely related to flow rate changes. There is no evidence of 6-hour periodicity or ~16-hour inertial band periodicity, indicating that tidal currents are not a factor.

References

- Baker, E. T. (1994), A 6-year Time Series of Hydrothermal Plumes Over the Cleft Segment of the Juan de Fuca Ridge. *J. Geophys. Res.* 99, 4889-4904.
- Bemis, K. G., R. P. Von Herzen, and M. J. Mottl (1993), Geothermal Heat Flux From Hydrothermal Plumes on the Juan de Fuca Ridge. *J. Geophys. Res.* 98, 6351-6365.
- Converse, D. R., Holland, H. D. & Edmond, J. M. (1984), Flow rates in the axial hot springs of the East Pacific Rise (21N): Implications for the heat budget and the formation of massive sulfide deposits. *Earth Planet. Sci. Lett.* 69, 159-175.
- Crone, T. J., and W. S. D. Wilcock (2005), Modeling the effects of tidal loading on mid-ocean ridge hydrothermal systems. *Geochem. Geophys. Geosyst.* 6(1), 1-25. doi:10.1029/2004GC000905.
- Elderfield, H. & Schultz (1996), A. Mid-ocean ridge hydrothermal fluxes and the chemical composition of the ocean. *Annu. Rev. Earth Planet. Sci.* 24, 191-224.
- Jupp, T. E., and A. S. Schultz (2004), A poroelastic model for the tidal modulation of seafloor hydrothermal systems. *J. Geophys. Res.* 109, doi:10.1029/2003JB002583.
- Mofjeld, H. O., F. I. Gonzales, and M. C. Eble (1995), Ocean tides in the continental margin off the Pacific Northwest Shelf. *J. Geophys. Res.* 100(C6), 10,789-10,800.
- Pruis, M. J. & Johnson, H. P. (2004), Tapping into the sub-seafloor: examining diffuse flow and temperature from an active seamount on the Juan de Fuca Ridge. *Earth Planet. Sci. Lett.* 217, 379-388.

Image Correlation Velocimetry

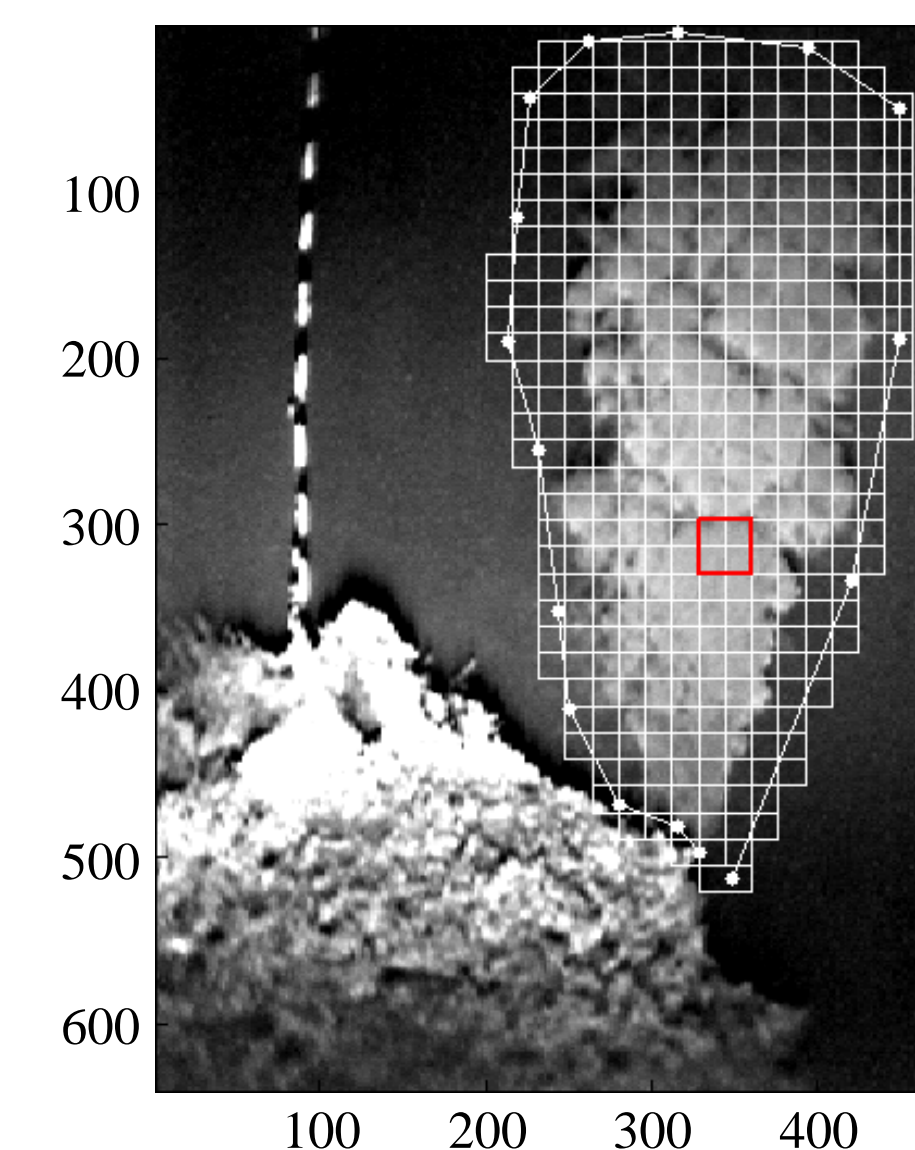


Figure 5. Typical frame grab showing the lower portion of a Main Endeavour Field black smoker plume extracted from video data collected in 1991. At left is a "scale mooring" indicating the approximate size of the imaged objects. Also shown is the grid of sub-images used in the image velocimetry technique. Each subimage from a video field is correlated with a subregion within a subsequent field.

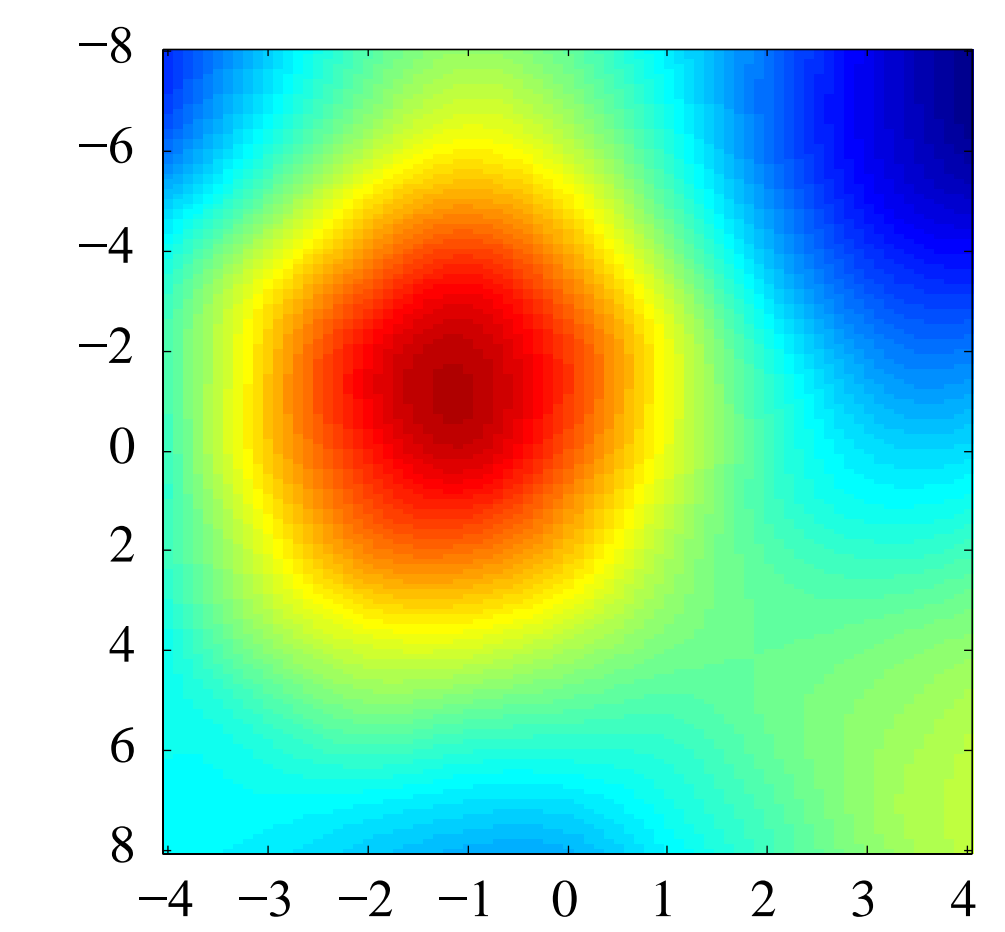


Figure 6. Colored contours of a typical two-dimensional cross-correlation function for a single subimage pair. This correlation function indicates that the flow structures in this part of the video frame moved ~1.3 pixels left and ~1.3 pixels up. We are currently working to establish meaningful confidence intervals for each cross-correlation in order to define an uncertainty for each velocity measurement.

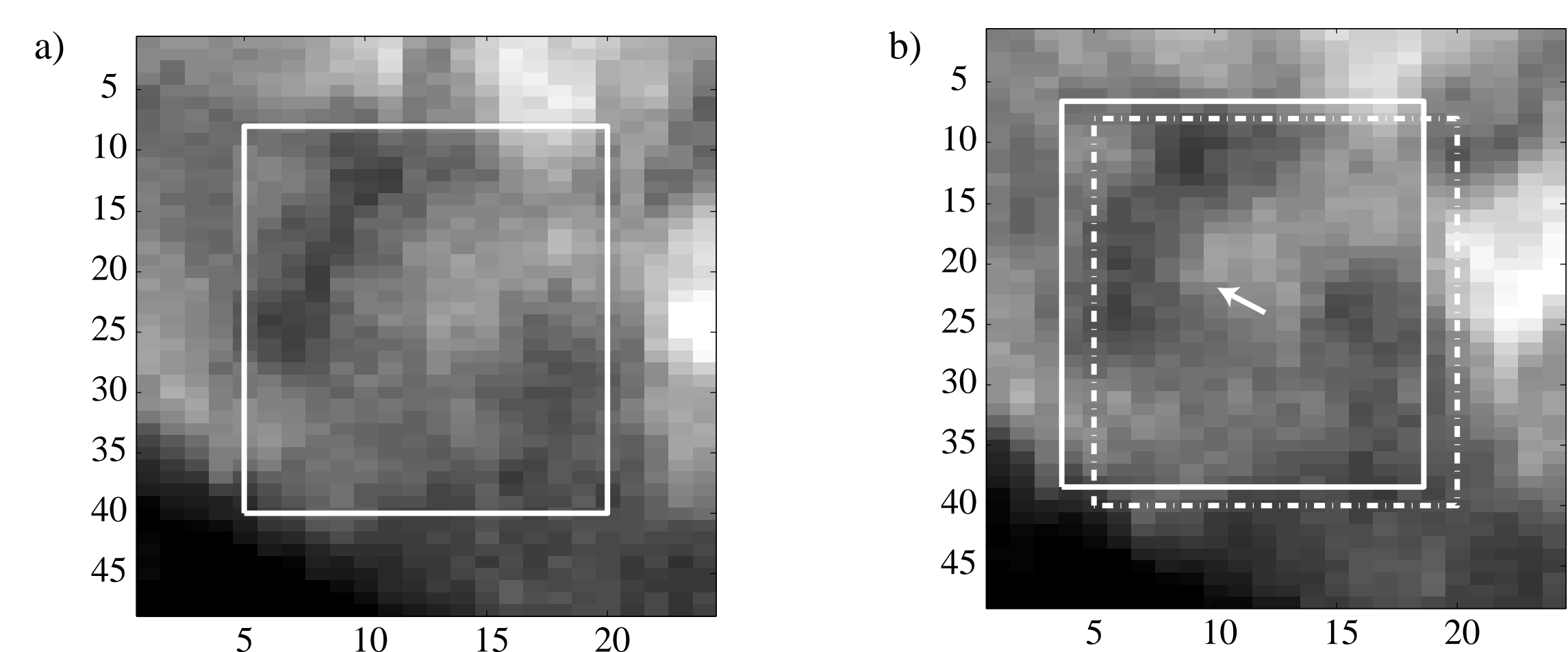


Figure 7. a) A single subimage defined by the white box; and b) its subimage pair showing the flow structure displacement from the two-dimensional cross-correlation. Image correlation velocimetry tracks the motions of flow structures (i.e. billows) within the turbulent plume to give an estimate of the "image-velocity" at a set of locations within the video frame. We are working to establish the optimal subimage size and frame interval for this technique. Variable subimage sizes may be required.

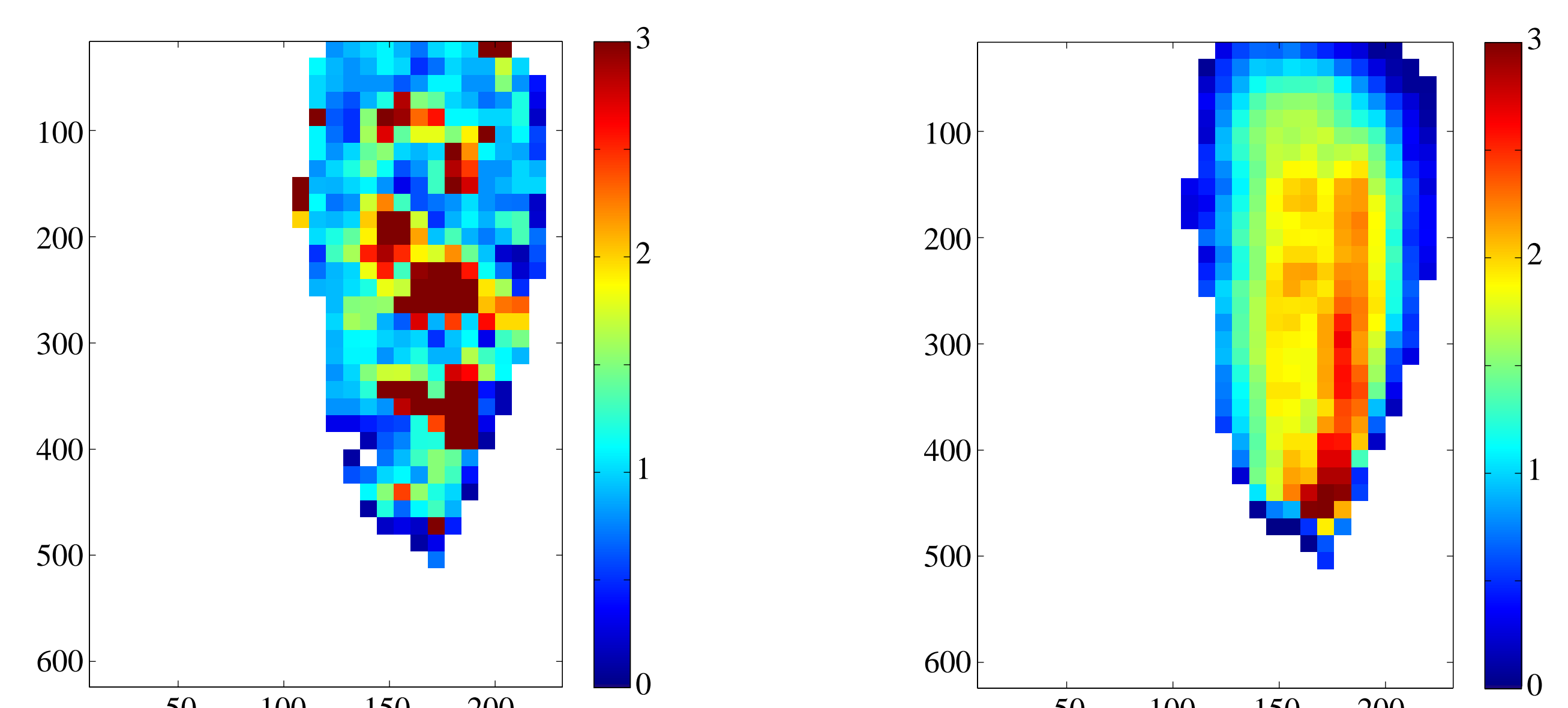


Figure 8. Colored contours of the image-velocity magnitude field for a single image pair. The scale is in pixels per 1/30 s. This image velocity magnitude field contains variations associated with turbulent flow variability as well as from noise from the technique. The clustering of velocity measurements suggests that much of the variability is real.

Figure 9. Colored contours of the time-averaged image-velocity magnitude field for one 30-s video clip (~1800 image pairs). Instantaneous flow variations and noise are smoothed out to reveal the expected Gaussian velocity distribution. Scale moorings (see Fig. 5) can be used to convert these measurements into calibrated velocities. We are currently working to characterize these average image velocity magnitude fields with a single representative flow rate.

Future Work

Black Smoker Acoustics:

- 1) Work to identify the sound source mechanisms operating within vents.
- 2) Deploy instrument with two hydrophones in September 2006.
- 3) Build hydrophone array capable of pinpointing the sound source location.
- 4) Obtain simultaneous sound and video measurements to cross-check the techniques.

Image Correlation Velocimetry:

- 1) Conduct laboratory experiment to image simulated hydrothermal jets with known flow rates.
- 2) Reduce noise by determining the optimum subimage sizes and frame interval, and establishing confidence intervals for the correlations.
- 3) Apply technique to previously collected video data from 1988, 1991, and 1995.
- 4) Build autonomous seafloor instrument.